A Study of two Dimensional Metal Carbide MXene Ti_3C_2

Synthesis, characterization conductivity and radiation properties

ZARRUL AZWAN MOHD RASID[1,2], MOHD FIRDAUS OMAR[1,2]*, MUHAMMAD FIRDAUS MOHD NAZERI[1,2], SYAHRUL AFFANDI SAIDI[3], ANDREI VICTOR SANDU[1,4]*, MUSTAFA AL BAKRI ABDULLAH MOHD[1]

[1]Centre of Excellence Geopolymer & Green Technology (CEGeoTech), School of Materials Engineering, Universiti Malaysia Perlis, Kompleks Pengajian Jejawi 2, 02600 Arau, Perlis, Malaysia

[2] School of Materials Engineering, Universiti Malaysia Perlis, Kompleks Pengajian Jejawi 2, 02600 Arau, Perlis, Malaysia

[3]Faculty of Engineering Technology, Universiti Malaysia Perlis, Uniciti Campus Sg Chucuh, 02100 Padang Besar, Perlis, Malaysia

[4] Gheorghe Asachi Technical University of lasi, Faculty of Materials Science and Engineering, Blvd. D. Mangeron 71, 700050, lasi, Romania

Since the discovery of exceptional properties of graphene, a lot of researchers focused on the discovery of another nobel two-dimensional (2D) materials. Recently, an elegant exfoliation approaches was proposed as a method to synthesis a new family of transitional 2D metal carbide or nitrades of MXene from a layered MAX phase. A layered MAX phase of Ti_3AlC_2 was synthesized through pressureless sintering (PLS) the initial powder of $3TiH_2/1.1Al/2C$ without preliminary dehydrogenation under argon atmosphere at 1350 ^oC. An elegant exfoliation approach was used to eliminates Al from its precursor to form a layered-structure of Ti_3C_2. In this study, thermal conductivity of MAX phase and MXene were studied using absolute axial heat flow method to measure the abilities sample to conduct heat and the data was collected using Picolog 1216 Data Logger. Electrical conductivity of these two materials was also compared by using two-point probe, due to its simplicity. Radiation properties of 2D MXene Ti_3C_2 was studied by using an established radon monitor, placed in closed, fabricated container. Morphological and structural properties of this 2D material were also studied using an established FESEM and XRD apparatus. SEM images shows two types of morphology which is a layer of Ti_3C_2 and the agglomerates Al_2O_3 with graphite. XRD pattern reveals three phases in this material which is a rhombohedral Al_2O_3, rhombohedral graphite and rhombohedral Ti_3C_2 phases, respectively. Thermal and electrical conductivity of MXene were proven higher than MAX phase. Radon concentration for this material for five consecutive days explains the radiation level of this material which is under the suggestion value from US Environmental Protection Agency (EPA). From this finding, it is can conveniently say that the MXene material can be promising material for electronic application.

Keywords: MXene, elegant exfoliation approach, pressureless sintering, radiation properties, conductivity

Two-dimensional (2D) materials are well known materials with unique properties in studies of materials engineering. 2D materials can be defines as a material with single atomic plane, such as graphene, with have only 0.34 nm thick of one atomic layer of carbon as shown in Fig.1[1]. Naguib et al. [1] state that 2D materials is known as a material with very high aspect ratio and thicknesses corresponding to a few atomic layers. In different studies, Bianco et al. [2] state that the range of materials to be 2D materials is 1 layer to 10 layers, and more than 10 layers is considered as 3D materials. By far the most studied 2D material is graphene, which is comprised of atomically thin layers of sp^2-bonded carbon atoms connected by aromatic in-plane bonds. Graphene is the first example of 2D materials with only one-atom thickness, isolated from graphite in 2004 by Novoselov et al. [3]. Since the outstanding electronic properties of graphene has been discovered, other 2D materials such as hexagonal boron nitrides [4], transition metal dichalcogenides (TMDs) [5], metal oxides, and hydroxides, have attracted much renewed attention.

Graphene shows tremendous attraction to researchers from different fields and has risen as the most exciting star in materials science during the past several years. Its exceptional properties, such as half-integer quantum Hall effect, ambipolar electric field effect, extremely high carrier mobility, high thermal conductivity, high specific surface area, and the highest strength ever measured, provide a fertile ground for the possible implementation of graphene in nano-devices for a large variety of applications, and a lot of recent reviews have been directed towards its synthesis, properties, and functionalized applications [6]. A fascinating idea was proposed by Naguib et al [7] which is to prepare freestanding graphene-like carbides (and nitrides) not from their 3D parent binary phases, but from ternary layered MAX phases (known also as nano-laminates), which include various 2D-like layers of transition metal carbides (or nitrides) as building blocks [8]. These 2D materials are now known as *MXenes*; this term denotes their genesis from MAX phases (with the

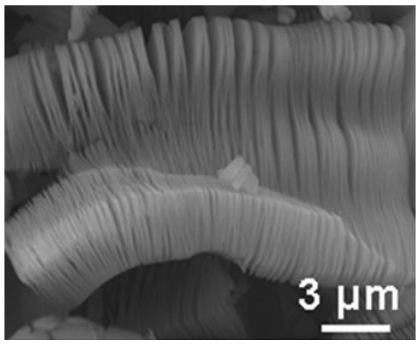

Fig 1. Scanning Electron Microscopy (SEM) images of 2D materials [1]

*email: firdausomar@unimap.edu.my ; sav@tuiasi.ro

loss of the A component) and their similarity to graphene [7].

MXenes is new 2D nanosheet materials and gaining so much attention from materials engineer because its properties and unique behaviour and has similar lamellar structure with graphene. Most of materials engineer is interested with new materials because the opportunity to become a new product with better technologies and application. Generally, 2D materials is produced by removing A from MAX phases by chemical etching as shown in Figure 1.2. MAX phases are ternary carbide or nitrides with the chemical formula of $M_{n+1}AX_n$, where M is an early transition metal, A is an A-group element and X is either carbon or nitrogen. The value of n can be 1, 2 or 3 [9].

Until recently, there is a limited number of work was discussed about the conductivity behaviour and the radon-222 (^{222}Rn) concentration of MXene. This two elements are important since this properties improves the practicality of this materials and long term exposure to radon is associated with lung cancer risk and present a significant environmental health hazard. Most of researchers studied the thermal and electrical conductivity of MXene using density functional theory (DFT) calculation, and this theoretical values does not illustrates the real conductivity properties since most of bulk sample contains a small defect or imperfection (Sumirat et al., 2006).^{222}Rn is the heaviest gas element, nine times heavier than air and a noble radioactive gas. This element does not chemically react with other materials in air and was occurs naturally from U-238 decay process. Inhalation of ^{222}Rn and ^{222}Rn daughter products for human will increase the possibility of lung cancer due to the presence of alpha (α) particles which have linear energy transfer (LET) and that affects the alveolus [10]. Measurements of radon are normally expressed as the concentration of radon in units of picocuries per liter of air (pCi/L) and the United States EPA recommendations are about 4 pCi/L or lower, which is the average or slightly above average for safety requirement in any applications [11-20].

To fullfill the lack of information in this specific area, we are proposely designed the synthesis method of MAX phase and MXene using a pressureless sintering technique and an elegant exfoliation approaches. For more comprehensive finding, the morphological, structural, thermal and electrical properties of MAX phase and MXene were intensively investigated and ultimately, the exhalation rate of radon (Rn) from MXene Ti_3C_2 were monitored using an established radon monitor, placed in closed, fabricated container.

Experimental part

Materials

Titanium hydrate (TiH_2, Alfa Aesar, United States), Aluminium (Al, ACROS ORGANICS, Austria) and graphite (C, ACROS ORGANICS, German) were used as raw materials to produce MAX phase. Hydrofluoric (HF, Qrec, New Zealand) solution was used as etchant to synthesis MXene from MAX phase.

Synthesis of MXene

The starting materials of TiH_2 (99 %, 325 mesh), Al (99 %, 200 mesh) and C (99 %, 550 mesh) was weighed according to the stoichiometry ratio of 3:1.1:2, then mixed by using a planetary ball mill for 60 hours. The powder was then cold-pressed to form a pellet with diameter of 1 cm and thickness of 0.3 cm before sintered in tube furnace by using a pressureless sintering (PLS) technique. The heating rate was controlled at 10°C/min and the sintering temperature was selected at 1350°C for 2 h in argon atmosphere. The pellet was then pulverized, immersed and stirred in HF (AR grade, 49 %, Qrec) for 20 hours in fume hood. The resulted mixture was then placed in centrifuge tube and centrifugation process was run at 5000 rpm for 7 minutes. The mixture was then washed with deionized water for several times, until the *p*H of solution approaching 7. The resulting Ti_3C_2 was then dried in vacuum at 50 ÚC for 24 h.

Characterization of MXene

X-ray diffraction (XRD) analysis was performed using Bruker D2 Phaser at 2θ values of 20-60° with Cu Kα radiation to determine the corresponding peaks of the MXene. X'pert HighScore Plus software was used to match the corresponding peaks with the standard data from International Committee of Diffraction Data (ICDD) X-ray data file. Morphological analysis was performed using Field Emission Scanning Electron Microscope (Nova NanoSEM 450) with an accelerating voltage of 10kv.

Thermal conductivity

Thermal conductivity test was carried out via absolute axial heat flow method to measure the abilities sample to conduct heat and the data was collected using Picolog 1216 Data Logger. The bulk sample was placed between two plates of hot and cold, respectively which connected in series. Heat was supplied to one side of the samples while a fully enclosed liquid cooling system was used on the other side creating a temperature gradient. The K-type thermocouple was used to record the temperature. Variable set of potential difference were applied to the sample within the range of 1.1 until 2.5 V. The obtained results used to plot the graph of power (Q) against temperature difference (ΔT). The slope of this graph was future implemented into the Eq. 1 to determine the thermal conductivity of the sample.

$$\mathbf{k} = \frac{\mathbf{Q} \times \mathbf{t}}{\Delta \mathbf{T} \times \mathbf{A}} \quad (1)$$

where, k is the thermal conductivity (W/mK), ΔT is the differences in temperature (°C), t is the specimen thickness (m), Q is the power (W), A is the specimen area (m^2)

Thermal conductivity

For electrical conductivity, two-point probe was selected as an implemented apparatus due to its simplicity. The sample was placed between two probes and by the application of constant 5.0 V to through the specimen, its conductivity can be measured. To obtain the conductivity of MAX phase compound, Ti_3AlC_2 and MXene phase compound, Ti_3C_2, the resistance need to be calculated first which follows the Eq. 2 and 3.

$$R = \frac{r \times A}{d} \quad (2)$$

$$\sigma = \frac{1}{R} \quad (3)$$

Where, R is the bulk resistivity, A is the area, D is the sample thickness, σ is the electrical conductivity

Radiation properties

A study of radiation properties is based on the measurement of radon concentration which was the exhalation rate of Rn from the sample. A bulk sample of MXene together with the professional radon monitor model 05-240, thermometer and hygrometer were placed in closed, fabricated container. The small openings of the

container were sealed by using modelling material. The build-up of Rn inside the container was measured using the radon monitor. Radon concentration was recorded every hour for five consecutive days. Data acquired includes the average and current radon concentrations (pCi/L), temperature (°C), relative humidity (%) and the time of sampling, respectively.

Results and discussions

Chracterization of MAX phase

Fig. 2 shows the comparison of XRD pattern that shows the effect of sintering towards the formation of MAX phase. Fig. 2 (before sintering) shows 3 phases which was detected before sintering which are TiO_2 (ICDD 00-034-0180), Ti_3AlC_2 (ICDD 00-052-0875) and cubic TiC (ICDD 00-006-0614) respectively. Among all of these phase, it can be clearly seen that cubic TiC and Ti_3AlC_2 were detected as dominant peak with the highest intensity at $2\theta = 35.74^o$.

The formation of new phase was detected after sintering shows the present phases were detected as rhombohedral Al_2O_3 (ICDD 01-075-0782), along with TiO_2, Ti_3AlC_2 and cubic TiC (ICDD 00-006-0614). TiC and Ti_3AlC_2 phase were detected as dominant phase along with Al_2O_3. The formation of oxide is attributed to the reaction between trapped oxygen in the tube furnace with Al which resulted alumina, Al_2O_3 in high temperature as shown in Eq. 4.

$$4Al + 3O_2 \rightarrow 2Al_2O_3 \quad (4)$$

Similar observation also found by [21] and describes the formation of Al_2O_3 as wear partner in the surface of Ti_2AlC. Apart from that, this phase analysis also shows the transition of Ti_3AlC_2 phase before and after sintering process. It can be seen that after sintering, the intensity of Ti_3AlC_2 increased and formed a single peak phase while the intensity and peak of TiC shows contrary trend. From this finding, it can be speculated that the Al was completely turns into liquid-phase during this process and combine with the Ti and graphite phase to form Ti_3AlC_2 phase.

Fig. 3 shows the morphological analysis of sample powder before and after sintering process. Before sintering process, sample powder shows irregular flakes-like shape as shown in Fig. 3 (a) with the thickness between 5 – 10 µm. This shape is the mixture of starting powders TiH_2/Al/C after milling process. Meanwhile, Fig. 3 (b) shows the morphological analysis of sample powder after sintering process and it can be seen that the shape of powder is totally changes to more compacted mixture and become more brittle, similarly with the result reported by Vitalariu et al. [22]. A layer of Ti_3AlC_2 and TiC was covered by oxide layer. The bond between particles is stronger since the purpose of sintering process is to impart the strength and the integrity of sample, as reported by German [23] which explained the sintering process improves the bonding strength and other engineering properties of compacted materials.

In Fig. 3 (b), the effect of sintering was clearly shown in the diagram where the Al phase turns into liquid phase and combine with the Ti and C phase, similar with the result reported by Argesanu et al. [24]. The microstructural in this diagram seen to be in one-bulk form of Ti, Al and graphite with the oxide phase from TiO_2 and Al_2O_3. This result was in line with Halim [25] which explained the morphological of MAX phase as a layered material where mechanical deformations take places by basal dislocations and is very anisotropic, which can lead to partial delamination and the formation of lamellae with the thicknesses ranging from 10 - 100 nm.

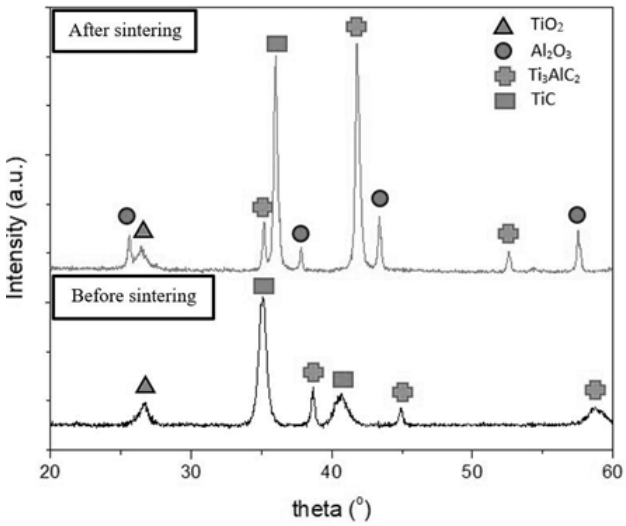

Fig. 2. XRD pattern shows the effect of sintering at 1350°C toward the formation of MAX phase, Ti_3AlC_2.

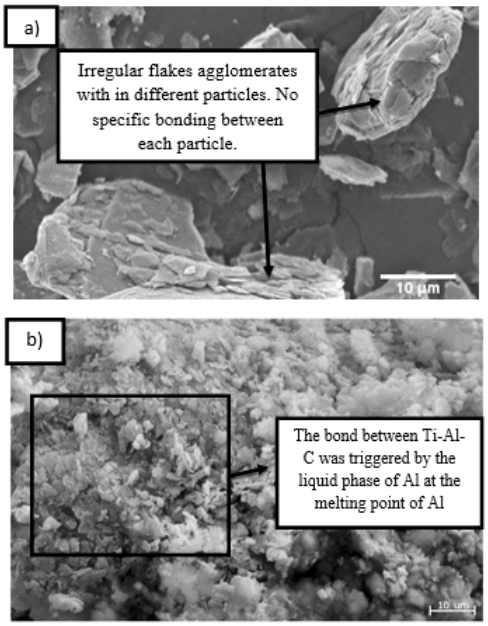

Fig. 3. Effect of sintering toward the formation of MAX phase, Ti3AlC2. (a) before sintering (b) after sintering.

The mechanism of this liquid-phase sintering in MAX phase was illustrated in Fig. 4 and in line with the one that been reported by Halim [25]. This statement also supported by Omura et al. [26] which scientifically proven that the reaction in TiC-Al system was triggered by the reaction between Ti and Al at melting point of Al, which around 660 °C.

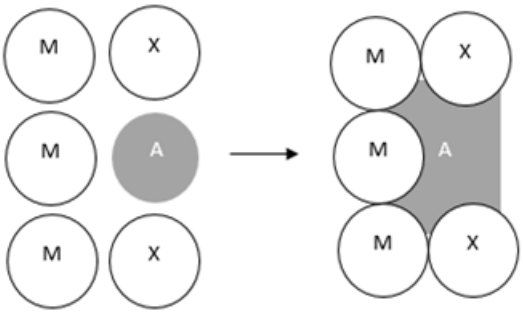

Fig. 4. The mechanism of MAX phase during sintering between Ti, Al and graphite phase.

Characterization of 2D MXene

Figure 5 shows the XRD pattern after a method an elegant exfoliation approaches was used. It was believed that Ti_3AlC_2 phase was fully vanished after chemical etched using a HF solution for 20 h and replaced by rhombohedral Ti_3C_2 phase.

The formation of Ti_3C_2 phase in XRD pattern instead of $Ti_3C_2(OH)_2$ in Eq. 6 is because the ultrasonication in methanol leads to exfoliation of MXene Ti_3C_2. This result is in line with reaction proposed by Naguib et al [7] where they reported the uses of aqueous hydrofluoric (HF) solution as etchant at room temperature. This process started when the Al atoms was replaced by O, OH and/or F atoms. The removal of Al atoms weakens the bond between M-X layers, allow them to separated. The reaction between MAX phase and HF solution produces aluminum fluoride (AlF_3), which are colorless solid precipitation. This reaction also produces hydrogen (H_2) bubbles as shown in Eq. 7. Resulting AlF_3 in Eq. 5 was eliminated during centrifugation process leaves the remaining Ti_3C_2 phase. Centrifugation was then performed to separate the solids, which were then washed with deionized water. The reactions of the HF solutions with Ti_3AlC_2 include:

$$Ti_3AlC_2 + 3HF \alpha AlF_3 + 3/2H_2 + Ti_3C_2 \quad (5)$$

$$Ti_3C_2 + 2H_2O \alpha Ti_3C_2(OH)_2 + H_2 \quad (6)$$

$$Ti_3C_2 + 2HF \alpha Ti_3C_2F_2 + H_2 \quad (7)$$

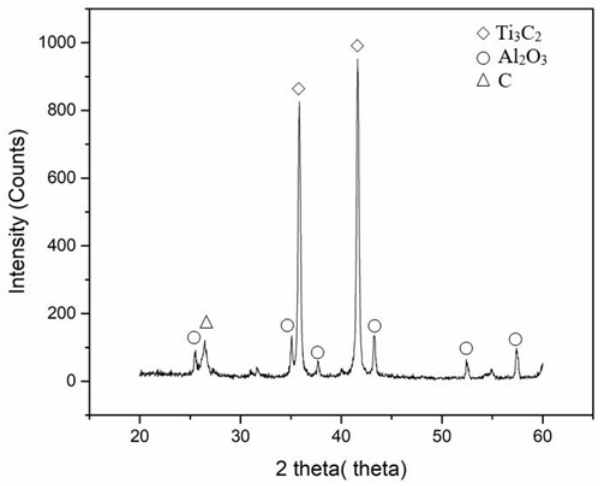

Fig. 5. X-ray diffraction pattern etching with 49% HF solution for 20 h

According to Walker & Garrett [27], even though the removal of Al occurred in MAX phase, the bond between MXene layers is weaker, but not weak enough to be broken by sonication process. Therefore, in order to breaks the bond between the layers and isolates the layer of Al and Ti-C, the intercalation of compound between layers was used. Fig. 6 shows SEM images after HF treatment, discovers two types of morphology which are a layer of Ti_3C_2 (marked as C) and the agglomerates Al_2O_3 with TiO_2. The images of layered Ti_3C_2 with the thickness of 0.1-0.3 µm confirms the successful exfoliation of Ti_3C_2 similar with reported exfoliation graphene by Naguib et al. [1].

The formation of MXene layers was illustrated in Fig. 7. The mechanism in this process involving an elegant exfoliation technique and sonication process. The bond between Ti-C in this reaction were contributed by Al in layers form. An elegant exfoliation technique is used to separates Al phase in this mixture. Al phase will react with HF solution and formed colorless solid precipitates known as AlF_3. Further sonication process separates this

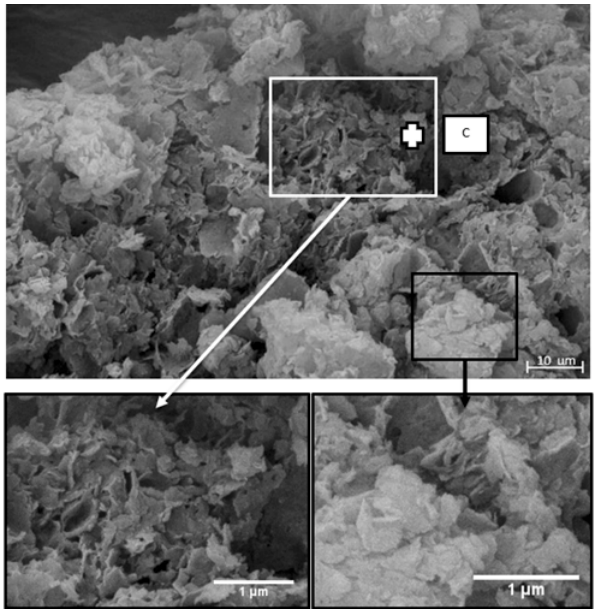

Fig. 6. SEM images for MXene after an elegant exfoliation approach with 49% HF solution

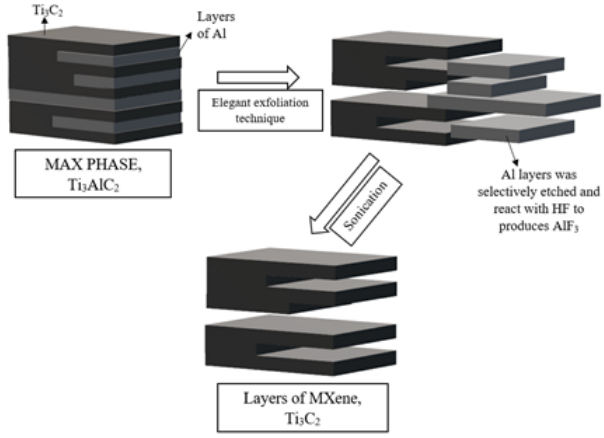

Fig. 7. Schematic diagram shows the mechanism during elegant exfoliation process

precipitates from the mixture and produces layers of MXene, Ti_3C_2.

Thermal and electrical conductivity

Fig. 8 shows the comparison between experimental and theoretical values of thermal conductivity between MAX phase and MXene. The thermal conductivity of MXene is proven higher than MAX phase. By comparing the experimental value and theoretical value, thermal conductivity of both MAX and MXene is lower since the theoretical measurement does not consider the porosity or defect of actual sample. This experimental thermal conductivity of MAX phase and MXene are 4.52 and 4.58 W/m.K, and the values are low compared to the thermal conductivity of single-layer graphene, which is around 6000 - 6000 W/m.K in room temperature [28]. However, this values was questioned for overestimated measurement by Yousefzadi Nobakht & Shin [29] and come out with the values of 1500 - 2500 W/m.K for suspended single layer of graphene. This range of values also obtained and verified by other researchers [30].

The comparison between theoretical and experimental values for electrical conductivities of MAX phase and MXene was presented in Fig. 9. This Figure also included the theoretical electrical conductivity of graphene, which were 26000 S/m. Similar with thermal conductivity, by comparing the experimental value and theoretical value,

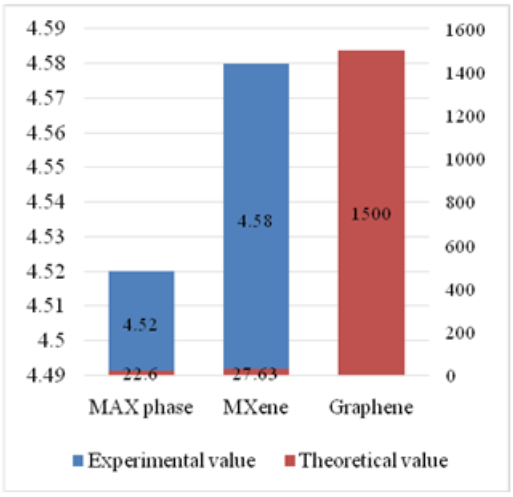

Fig. 8. Theoretical and experimental value of thermal conductivity between MAX phase and MXene

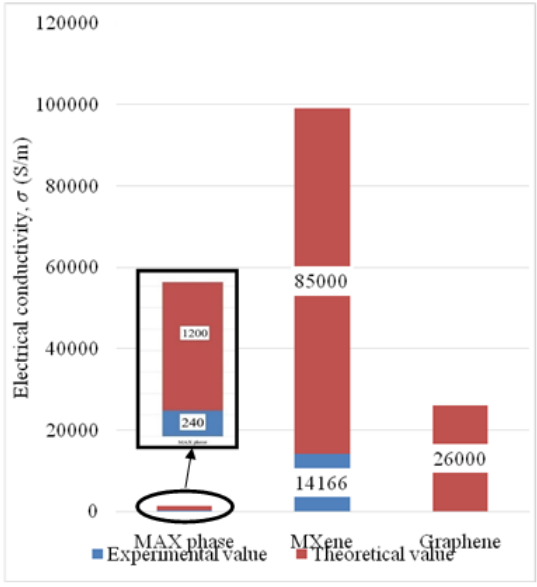

Fig.9. Theoretical and experimental value of electrical conductivity between MAX phase, MXene and graphene.

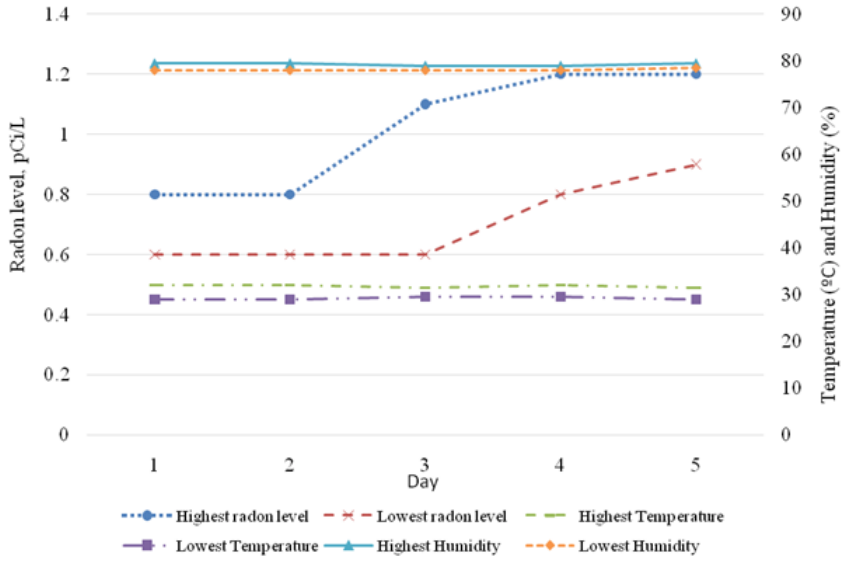

Fig. 10. Radon concentration of MXene phase compound Ti_3C_2 for five consecutive days.

electrical conductivity of both MAX and MXene is lower since the theoretical measurement does not consider the porosity or defect of actual sample. The difference in conductivities values of theoretical and experimental happen due to percolation behaviour and the reduction in the number of charge carriers. The interaction between pure MXene and the void, such as Al_2O_3 blocked the conductive network, by considering the properties of Al_2O_3 as electrical insulator, and affects the electrical conductivity of MXene. According to Sumirat et al.[31], thermal and electrical conductivity decreased with the increasing porosity because of effective phonon scatterings by pores. Porosity in bulk sample containing a gas, such as air in the pores affect the sample by adding an insulation character to the bulk sample.

Radiation properties

Fig. 10 shows the radon concentration properties of 2D MXene Ti_3C_2 and the rate of radon was slightly increase started from day 2 to day 5.The highest radon concentration was recorded at day 5, which was 1.2 pCi/L and this value is lower that the suggested value by United State Environmental Protection Agency (EPA), which was 4 pCi/L. Humidity and temperature inside of the chamber was maintained between 78.0 -79.5 % and 29 -32ºC. Hence, it was experimentally proven that Ti_3C_2 could be an alternative material towards the development of new electronic technologies due to small radiation emission and considered safe for consumer usage.

Conclusions

This study was devoted to assess the thermal and electrical conductivities of MAX phase and 2D MXene, along with the radiation properties of 2D MXene. From the finding, it can be concluded that the MAX phase and MXene was susscessfully sunthesized using an elegant exfoliation approaches. The structural and morphological of both MAX phase and MXene phases was confirmed by XRD and SEM assessment. There are three phases was detected by XRD after the treatment which is Ti_3C_2 and the agglomerates of C and Al_2O_3. SEM image shows the agglomerates of this phase at the side of Ti_3C_2 layers. Thermal and electrical conductivity of MXene is experimentally proven higher than MAX phase, but lower than theoretical value. Radon concentration for this material for five consecutive days explains the radiation level of this material is under the suggestion value from US Environmental Protection Agency (EPA). From this finding, it can be concluded that this materials is promising material for electronic application.

Acknowledgement.This present work was carried out at Universiti Malaysia Perlis and supported by Ministry of Higher Education of Malaysia under the Fundamental Research Grant Scheme (FRGS) number 9003-00390.

References

1.NAGUIB, M., COME, J., Electrochem. Commun., **16**, 2012, p.61
2.BIANCO, A., CHENG, H.M., Elsevier, 2013
3.NOVOSELOV, K.S., GEIM, A.K., MOROZOV, S.V., JIANG, D., ZHANG, Y., DUBONOS, S.V., GRIGORIEVA, I.V., FIRSOV, A.A., 2004, p.666
4.HAUBNER, R., WILHELM, M., WEISSENBACHER, R., LUX, B. Springer, 2002, p.1
5.MIRO, P., GHORBANI-ASL, M.,HEINE, T., Angewandte Chemie International Edition, **53**,2014, p.3015.
6.TANG, Q., ZHOU, Z., Prog. Mater. Sci., **58**, 2013, p.1244
7.NAGUIB, M., KURTOGLU, M., PRESSER, V., LU, J.,NIU, J.,HEON, M., HULTMAN, L., GOGOTSI, Y.,BARSOUM, M.W., Adv. Mat. **23**, 2011, p.4248
8.SHEIN, I.R., IVANOVSKII, A.L., Micro Nano Lett., **8**, 2013, p.59
9.NAGUIB, M., MASHTALIR, O., CARLE, J., PRESSER, V., LU, J.,HULTMAN, L., GOGOTSI, Y.,BARSOUM, M.W., **6**, 2012, p.1322
10.SAIDI, S.A., JAAFAR, M.S., RAZAB, A., AZHAR, M.K.,RASAT, M.,SUKHAIRI, M., AHMAD, M.I., MOHAMED, M., MAMAT, S., HUSSIN, H., Mat. Sci. Forum, 2016, p. 427
11.SAIDI, S.A., JAAFAR, M.S., RAZAB, A., ZULKEPLI, N.N., Aust. J. Basic & Appl. Sci., **7**, 2013, p.315
12.BOJAN, A.C., POPA, A.G., PUSKAS, A., Procedia Engineering, **181**, 2017, p. 712.
13.CORBU, O., POPOVICI, A., POPITA, G.E., RUSU, T., ROSU, C., PUSKAS, A., International Multidisciplinary Scientific GeoConference-SGEM, 2014, p. 81.
14.BERE, P., DUDESCU, M.C., BALC, N., BERCE, P., IURIAN, A.M., NEMES, O., Mat. Plast., **51**, no. 2, 2014, p. 145.
15.KOLLO, S.A., KOLLO, G., PUSKAS, A., Procedia Technology, **22**, 2016, p. 312.
16.VIZUREANU, P., PERJU, M.C., GALUSCA, D.G., NEJNERU, C., AGOP, M., Metalurgia International, 15, no. 12, 2010, p. 59.
17.ACHITEI, D.C., VIZUREANU, P., DANA, D., CIMPOESU, N., Metalurgia International, **18**, special issue 2, 2013, p. 104.
18.FLOREA, C.D., CARCEA, I., CIMPOESU, R., TOMA, S.L., SANDU, I.G., BEJINARIU, C., Rev. Chim. (Bucharest), **68**, no. 10, 2017, p. 2397.
19.BEJINARIU, C., DARABONT, D.C., BACIU, E.R., GEORGESCU, I.S., BERNEVIG-SAVA, M.A., BACIU, C., Sustainability, **9**, no. 7, 2017, art. 1263.
20.DRAGOMIR, C.S., MEITA, V., DOBRE, D., GEORGESCU, E.S., BORCIA, I.S., Present Environment And Sustainable Development, **9**, no. 2, 2015, p.113.
21.GUPTA, S., FILIMONOV, D., PALANISAMANY, T., BARSOUM, M., Wear, **265**, 2008, p.560
22.VITALARIU, R., LEATA, R.,CHELARIU, R., MUNTEANU, C., CIMPOESU, R., ILIE, M., COMANECI, R., MOISEI, M., Rev. Chim.(Bucharest), **66**, 2015
23.GERMAN, R.M., Sol.-Terr. Phys, 1996, p.568.
24.ARGESANU, C., BOMBOS, D., MATEI, V., JUGANARU, T., BOMBOS, M., VASILIEVICI, G., Rev. Chim.(Bucharest), **65**, 2014, p.1391
25.HALIM, J., Linköping University Electronic Press, 2014
26.OMURA, N., KOBASHI, M., CHOH, T., KANETAKE, N., J. Japan. Inst. Met., 66, 2002, p.1317.
27.WALKER, G., GARRETT, W., Sci., 156, 1967, p.385
28.BALANDIN, A.A., GHOSH, S., BAO, W., CALIZO, I., TEWELDEBRHAN, MIAO, F., Nano Lett., 8, 2008, p.902.
29.YOUSEFZADI NOBAKHT, A., SHIN, S., J. Appl. Phys., **120**, 2016, p. 225111
30.FAUGERAS, C., FAUGERAS, B., ORLITA, M., POTEMSKI, M., NAIR, R.R., GEIM, A., ACS Nano, **4**, 2010, p.1889
31.SUMIRAT, I., ANDO, Y., SHIMAMURA, S., J. Por. Mater., **13**, 2006, p.439

Manuscript received: 15.06.2019